Sciencexpress Report

# The Radiative Signature of Upper Tropospheric Moistening

Brian J. Soden,[1]* Darren L. Jackson,[2] V. Ramaswamy,[3] M. D. Schwarzkopf,[3] Xianglei Huang[4]

[1]Rosenstiel School for Marine and Atmospheric Science, University of Miami, Miami, FL 33149, USA. [2]Cooperative Institute for Research in Environmental Sciences, University of Colorado, Boulder, CO 80305, USA. [3]Geophysical Fluid Dynamics Laboratory, National Oceanic and Atmospheric Administration, Princeton, NJ 08542, USA. [4]Atmospheric and Oceanic Sciences Program, Princeton University, Princeton, NJ 08542, USA.

*To whom correspondence should be addressed. E-mail: bsoden@rsmas.miami.edu

**Climate models predict that the concentration of water vapor in the upper troposphere could double by the end of the century as a result of increases in greenhouse gases. Such moistening plays a key role in amplifying the rate at which the climate warms in response to anthropogenic activities but has been difficult to detect because of deficiencies in conventional observing systems. We use satellite measurements to highlight a distinct radiative signature of upper tropospheric moistening over the period 1982 to 2004. The observed moistening is accurately captured by climate model simulations and lends further credence to model projections of future global warming.**

The importance of water vapor in regulating climate is undisputed. It is the dominant greenhouse gas, trapping more of Earth's heat than any other gaseous constituent (*1*). As the climate warms in response to increases in other greenhouse gases such as carbon dioxide, the concentrations of water vapor are expected to increase (*2–7*). If water vapor concentrations do increase in a warmer world, the added absorption will act to further amplify the initial warming. Models of Earth's climate suggest that this serves as a powerful positive feedback, more than doubling the sensitivity of the surface temperature to an anthropogenic forcing (*8–11*).

All climate models predict that the concentration of water vapor in the upper troposphere will increase dramatically in the future (*9*, *12*). However the validity of such projections has been debated for over a decade (*13*, *14*). Some argue that the concentrations in the upper troposphere might actually decrease in a warmer climate, noting the simplified treatment of convection and cloud-related processes in current models and the important role that they play in governing the distribution of moisture (*15–17*).

Here we use climate model simulations and satellite measurements to demonstrate the presence of a distinct radiative signature of upper tropospheric moistening on interannual to decadal time scales. The observed moistening is consistent with model simulations and corresponds approximately to a constant relative humidity increase in upper tropospheric moisture (*18*). We further demonstrate that without such an increase, the model would be unable to reproduce the satellite-observed radiance record.

The distribution of water vapor is highly variable in both space and time. Because the equilibrium vapor pressure of water depends strongly on temperature, the concentration of water vapor diminishes rapidly with height. Yet because the absorptivity of water vapor is proportional to the logarithm of its concentration, it is the fractional change in water vapor mass, not the absolute change, which governs its strength as a feedback mechanism.

Model calculations of the fractional change in global-mean water vapor mixing ratio (*19*) using the Geophysical Fluid Dynamics Laboratory (GFDL) atmospheric general circulation model (*20*) indicate a distinct upper tropospheric amplification to the simulated changes in water vapor over the past two decades (*21*) (fig. S1). A similar vertical amplification is predicted to occur over the coming century in response to increases in anthropogenic greenhouse gases and is a robust feature of all climate model projections (*9*, *12*, *18*). Simulations of the 21st century climate using the GFDL coupled ocean-atmosphere model indicate an increase in lower tropospheric water vapor of ~20% by the end of the century, but an upper tropospheric increase of ~100% (*21*) (fig. S1). Such dramatic moistening highlights the significance of upper tropospheric water vapor as a feedback mechanism and underscores the importance of its measurement to the detection and attribution of climate change.

Previous studies have demonstrated the presence of regional moistening trends in the lower troposphere since the mid-1970s from radiosonde measurements (*22*, *23*). Increases in the total column water vapor mass (*19*) have also been observed over the global oceans since the mid-1980s from satellites (*24*, *25*). These lower tropospheric moistening

trends are strongly linked to changes in surface temperature and are consistent with that expected under the assumption of constant relative humidity.

The model used here is an atmospheric general circulation model (GCM) integrated with specified sea surface temperatures (*20*). Four sets of model integrations are performed, each starting in January of 1982, when satellite-observed SSTs become available, and ending in December 2004. Because the global anomalies of the ensemble members are nearly identical, only the results from the first member are displayed in the figures, but the trends and standard errors of the trends for all members are summarized in Table 1 (*26*).

When forced with observed sea-surface temperatures, this model successfully reproduces the observed column integrated moistening changes over this period (Fig. 1). However, because the mass of water vapor decreases rapidly with height, the column integral is primarily weighted by the lower troposphere and its largely thermodynamic behavior is unsurprising (*21*). Consequently, the projected increase of column integrated water vapor in response to global warming is of little debate and its agreement with models provides only limited reassurance in their simulation of water vapor feedback (*9*).

In contrast, water vapor in the free troposphere is not so directly constrained by thermodynamic arguments (*21*) and its response to global warming has been the subject of long-standing controversy (*9*, *15–17*). Given the radiative importance of moisture changes in the upper troposphere (*9*, *10*), it is important that humidity changes there are demonstrably consistent between models and observations. Although an international network of weather balloons has carried water vapor sensors for over half a century, changes in instrumentation and poor calibration make such sensors unsuitable for detecting trends in upper tropospheric water vapor (*27*). Similarly, global reanalysis products also suffer from spurious variability and trends related to changes in data quality and data coverage (*24*).

Satellite observations using the High Resolution Infrared Radiometer Sounder (HIRS) provide a global, temporally-coherent archive of radiance measurements in the 6.3 μm water vapor absorption band from 1979 to the present. The radiance channel centered at 6.7 μm (channel 12) is sensitive to water vapor integrated over a broad layer of the upper troposphere (200 to 500 hPa) and has been widely used for studies of upper tropospheric water vapor (*28*). Since clouds strongly attenuate the infrared radiation, we restrict our analysis to clear-sky radiances in which the upwelling radiation in channel 12 is not affected by clouds (*29*).

Figure 2 compares the satellite-observed equivalent blackbody temperatures from channel 12 (T12) from the HIRS instrument with those computed from the model's temperature and moisture profiles (*30*). Under clear skies, T12 is primarily sensitive to changes in relative humidity averaged over a deep layer of the upper troposphere (roughly 200 to 500 hPa) (*21*). Thus, if the water vapor mass in the upper troposphere decreases by conserving relative humidity as the atmosphere cools, only a small perturbation to T12 would be expected.

While significant trends in T12 do occur regionally (*31*, *32*), the globally averaged radiance record from HIRS shows little trend over the 20 year period. This lack of trend is consistent with that derived from previous studies (21, *33–36*) and insensitive to the intercalibration of the radiance records from individual satellites (*21*). The model simulations also yield little trend in global-mean T12, implying that there is little change in global mean relative humidity over this period. In fact, the model-simulated anomalies are nearly identical to those obtained if one repeats the calculation of T12 under the assumption of a constant relative humidity change in the model's water vapor field (*21*). This confirms that both the observations and GCM simulations are, to first order, consistent with a constant relative humidity behavior.

In contrast, consider the trend in T12 that would result if there was no increase in water vapor mass in the model's upper troposphere (shown as a green curve in Fig. 2A) (*21*). In this case, the T12 would increase by more than 0.5 K over the period from 1982 to 2000, more than four times what was observed, due to an increase in Planck emission (warming) without a compensating increase in atmospheric attenuation (moistening). This discrepancy is much larger than the standard error in the trend estimates and is consistent across all GCM ensemble members (Table 1). Thus the model would be unable to reproduce the observed radiance record without a nearly constant relative-humidity moistening of the upper troposphere.

Because the anomalies in T12 are a function of both moisture and temperature changes over this period, it is important to verify the credibility of the model-simulated temperature variations. For this purpose, the global-mean tropospheric temperature anomalies observed from the Microwave Sounding Unit (MSU) channel 2 radiances (T2) are compared with those simulated from the GCM (Fig. 2B). The MSU T2 radiances are primarily sensitive to the temperature averaged over a deep layer of the troposphere (roughly 200 to 800 hPa). Observations are shown for both the University of Alabama-Huntsville (UAH) (*37*) and Remote Sensing Systems (RSS) (*38*) versions of MSU channel 2. Over the period 1982 to 2004, the GCM-simulated T2 anomalies are nearly identical in pattern to those observed from MSU regardless of which record is used. The linear trend of the GCM-simulated T2 (0.18 K/decade) (*21*) is in close agreement with the RSS T2 trend (0.17 K/decade). However, both the GCM and RSS trends are roughly a factor

of 2 larger than the UAH trend, reflecting differences between the UAH and RSS reconstruction methods (*38*).

The trend in upper tropospheric water vapor are more easily depicted by differencing the global-mean MSU channel 2 and HIRS channel 12 radiance measurements (T2-T12). As the atmosphere moistens, the emission level for T12 increases due to the increasing opacity of water vapor along the satellite line of sight. On the other hand, because the concentration of oxygen does not vary by any appreciable amount, the emission level for the MSU T2 remains constant. Therefore, if the atmosphere moistens, the brightness temperature difference T2-T12 will increase over time due to the divergence of their emission levels. If, on the other hand, the moisture in the upper troposphere does not increase, the emission level for T12 would remain unchanged and T2-T12 would show little change over time.

Both the HIRS observations and GCM simulations indicate an increase in T2-T12 over this period, reflecting the moistening of the upper troposphere (Fig. 2C). The model-simulated anomalies in T2-T12 increase at a rate of 0.14 K/decade from 1982 to 2004. However, if the concentrations of water vapor are held constant when computing the model's T12, (green curve in Fig. 2C) the trend in T2-T12 becomes negative (–0.04K/decade), in stark contrast with that observed.

Both RSS (0.16) and UAH (0.08) reveal increases in T2-T12 over this period (Fig. 2C), although the magnitude of the linear trend is roughly twice as large when using RSS T2 than using UAH T2, reflecting the uncertainty in the rate at which the troposphere has warmed over this period (*38*, *39*). However it is important to note that while the linear trends differ between the UAH and RSS T2, both show similar variability at lower frequencies and that this variability is consistent with a moist-adiabatic warming (*40*) and constant relative humidity moistening of the upper troposphere. In contrast, the "no moistening" version of the model radiance simulations is unable to capture the either the observed variability or the linear trend in T2-T12.

The zonal mean of the trend in T2-T12 (Fig. 3) further highlights the consistency between the observed and GCM-simulated radiance record with both showing largest increases in upper tropospheric water vapor in the tropics and smaller decreases near the poles, including a local maximum in the northern subtropics between 0-30N. In contrast, the zonal-mean trends in T2-T12 for the "no moistening" scenario is negative in most latitudes, in stark contrast to either the HIRS/RSS or HIRS/UAH record. Note that there are regions where the model simulated trend of T2-T12 departs significantly from the constant relative humidity approximation, the cause of which warrant further scrutiny.

Upper tropospheric water vapor provides a powerful feedback for amplifying climate change and its increase is a crucial ingredient to model projections of future global warming. An accurate understanding of the changes in upper tropospheric moisture over time is necessary to verify its role in amplifying climate sensitivity. We use satellite measurements to highlight a distinct radiative signature of upper tropospheric moistening on interannual to decadal time scales over the period 1982 to 2004. To reproduce the observed radiance record requires a global moistening of the upper troposphere in response to atmospheric warming that is roughly equivalent in magnitude to that predicted under the assumption of constant relative humidity. This behavior is consistent with that simulated from current models and provides key quantitative evidence in support of their ability to predict the climate feedback from upper tropospheric water vapor. Given the importance of water vapor feedback in determining the climatic response to anthropogenic forcings, such confirmation is essential to the use of these models for global warming projections.

**References and Notes**


1. J. Kiehl, K. Trenberth, *Bull. Am. Meteorol. Soc.* **78**, 197 (1997).
2. U. Cubasch, R. Cess, in *Climate Change: The IPCC Scientific Assessment*, J. T. Houghton *et al.*, Eds. (Cambridge Univ. Press, Cambridge, 1990).
3. R. Cess *et al*., *J. Geophys. Res.* **95**, 16601 (1990).
4. A. Raval, V. Ramathan, *Nature* **342**, 758 (1989).
5. R. Pierrehumbert, *J. Atmos. Sci.* **52**, 1806 (1995).
6. D. Rind *et al*., *Nature* **349**, 500 (1991).
7. A. Del Genio, W. Kovari, Y. Mao-Sung, *Geophys. Res. Lett*. **21**, 2701 (1994).
8. T. Stocker *et al.*, in *Climate Change 2001: Contribution of Working Group I to the Third Assessment Report of the Intergovernmental Panel on Climate Change* (Cambridge, UK: Cambridge Univ. Press, 2001), pp. 418–470.
9. I. Held, B. Soden, *Ann. Rev. Energy Environ*. **25**, 441 (2000).
10. R. Colman, *Geophys. Res. Lett*. 31, L21109, doi:10.1029/2004GL020708 (2004).
11. R. Wetherald, S. Manabe, *J. Atmos. Sci*. **45**, 1397 (1988).
12. B. Soden *et al*., *Science* **296**, 727 (2002).
13. R. Lindzen, *Bull. Am. Meteorol. Soc.* **71**, 288 (1990).
14. R. E. Dickinson *et al.*, in *Climate Change 1995: The Science of Climate Change*, J. T. Houghton *et al.*, Eds. (Cambridge Univ. Press, Cambridge, 1996).
15. D. Sun, R. Lindzen, *J. Atmos. Sci*. **50**, 1644 (1993)
16. R. Lindzen *et al.*, *Bull Am. Meteorol. Soc*. **82**, 417 (2001)
17. K. Minschwaner, A. Dessler*, J. Climate* **17**, 1272 (2003).
18. Under a constant relative humidity, the concentration of water vapor is determined by changes in the equilibrium vapor pressure which increases rapidly with temperature. The Clausius-Clapeyron equation dictates that the fractional increase in equilibrium vapor pressure (es)

scales according to $dlne_s/dT \sim 1/T^2$. Near the surface this would lead to roughly a 6% increase in water vapor mass per 1 K warming. In the upper troposphere, where temperatures are colder, the water vapor mass increases at roughly twice this rate (*9*).

19. The water vapor mixing ratio (w) is defined as the mass of water vapor per unit mass of dry air. The relative humidity (r) is determined as the ratio of the water vapor mixing ratio to its "saturated" or equilibrium value ($w_s$), expressed in percent; $r=100*w/w_s$. The total column water vapor (W) is defined as the vertically integrated mass of water vapor per unit area in units of $kg/m^2$; $W = \int w \rho dz$ where ρ is the density of air and z is altitude and the integration is performed from the surface to the top of the atmosphere.
20. Model simulations are from the GFDL atmospheric general circulation model integrated with observed ocean sea temperatures (SSTs); see Anderson *et al*., *J. Climate* **17**, 461 (2004) for a description of the atmospheric model and SST data set.
21. See supporting online material at *Science* Online.
22. R. Ross, W. Elliott, *J. Climate* **14**, 1602 (2001)
23. P. Zhai, R. Eskridge, *J. Climate* **10,** 2643 (1997)
24. K. Trenberth, J. Fasullo, L. Smith, *Climate Dyn*., **24**, 741758, doi:10.1007/s00382-005-0017-4 (2005)
25. F. Wentz, M. Schabel, *Nature* **403**, 414 (2000).
26. A statistical model (E. C. Weatherhead *et al.*, *J. Geophys. Res*. **103**, 17149, 1998) was used to determine the standard errors of the trends in Table 1. An estimate of the trend (ω) for each time series was determined using a least squares linear fit. The residual time series, $N_t$, is defined as the residual time series following removal of the mean, the annual cycle, and the linear trend from the original time series. If we define the variance of $N_t$ as $\sigma_N^2 = Var(N_t)$ then the standard deviation of the trend can be approximated using equation (2) from Weatherhead *et al*. as $\sigma_\omega \cong \frac{\sigma_N}{n^{3/2}} \left( \frac{1+\phi}{1-\phi} \right)^{1/2}$ where the lag-1 autocorrelation is defined as $\phi = Corr(N_t, N_{t-1})$ and n defines the number of years in the monthly mean time series. Table 1 provides $\omega +/- 2\sigma_\omega$ for each time series. A trend may be considered to meet the 95% confidence level when $|\omega| > 2\sigma_\omega$.
27. W. Elliott, D. Gaffen, *Bull. Amer. Meteor.* Soc. **72**, 1507 (1991).
28. B. Soden, F. Bretherton, *J. Geophys. Res.* **98,** 16669 (1993).
29. We use an updated set of clear-sky radiances from HIRS as described in (32). While there could be deficiencies in the cloud-screening methodology which might bias the observed T12, the most recent analysis of cirrus clouds from HIRS using a method specifically designed to detect thin cirrus indicates no discernible trend in high level cloud cover over the period of record (Wylie *et al.*, *J. Climate*, in press).
30. To avoid uncertainties associated with the inversion of satellite-measured radiances into geophysical quantities, the GCM profiles of temperature and water vapor mixing ratio were input into a narrow band radiative transfer model to simulate the T12 which the HIRS instrument would observed under those conditions. The radiative transfer model used here is the HIRS Fast Forward Program (HFFP); B. Soden *et al*., *Bull. Am. Meteorol. Soc*. **81**, 797 (2000).
31. J. Bates, X. Wu, D. Jackson, *J. Clim*. **9**, 427 (1996);
32. J. Bates, D. Jackson, *Geophys. Res. Lett*. **28**, 1695 (2001).
33. B. Soden, R. Fu, *J. Climate* **8**, 2333 (1995).
34. A. Geer, J. Harries, H. Brindley, *J. Climate* **12**, 1940 (1998).
35. R. Allan, M. Ringer, A. Slingo, *Q. J. R. Meteorol. Soc*. **128**, 1 (2003).
36. M. McCarthy, R. Toumi, *J. Climate* **17**, 3181 (2004).
37. J. Christy, R. Spencer, W. Braswell, *J. Atmos. Oceanic Tech*. **17**, 1153 (2000).
38. C. Mears, M. Schabel, F. Wentz, *J. Climate* **16**, 3650 (2003).
39. C. Mears, F. Wentz., *Science* doi: 10.1126/science.1114772 (2005).
40. B. Santer *et al*., *Science* doi: 10.1126/science.1114867 (2005).
41. This research was partially supported by the NOAA Office of Global Programs.

**Supporting Online Material**

www.sciencemag.org/cgi/content/full/1115602/DC1
SOM Text
Fig. S1
References

1 June 2005; accepted 29 September 2005
Published online 6 October 2005; 10.1126/science.1115602
Include this information when citing this paper.

**Fig. 1.** The global mean (ocean-only) anomalies in column integrated water vapor from GFDL atmospheric GCM simulations forced with observed sea surface temperatures (*20*; red) and satellite observations from SSMI (*25*; black).

**Fig. 2.** The global mean time series of T12 (top), T2 (middle) and T2-T12 (bottom) from GCM simulations (red) and satellite observations (black). The model simulated radiances are also shown from calculations using a seasonally-varying climatological profile with no moistening trend (green line;

*21*) and a prescribed moisture profile which moistens at a constant relative humidity rate (red dashed line; *21*). All time series are smoothed using a 6-month running mean.

**Fig. 3.** An area-weighted projection of the zonal mean of the local trend in T2-T12 (K/decade) for satellite observations (black) and GCM simulations (red). The corresponding trends in T2-T12 for model simulated radiances under the constraint of no moistening (green line; *21*) and constant relative humidity moistening (red dashed line; *21*) are also shown.

**Table 1.** The linear least-squares trend ±2 standard errors of the linear trend for satellite observations and climate model simulations of total column water vapor, T12, T2, and T12-T2. The standard errors are estimated following Weatherhead *et al*. (*26*). The right hand column depicts the trends for which the GCM-simulated T12 was computed under the "no moistening" scenario (*21*). Satellite observed trends are computed using the SSMI total column water vapor (*25*), HIRS T12 (*21*), and MSU T2 for both RSS (*38*) and UAH (*37*). GCM trends are shown for each of the four model ensemble members. Bold indicates results shown in Figs. 1 and 2.

| | Satellite | GCM | GCM (no moistening) |
|---|---|---|---|
| total column vapor (%/decade) | 1.40 ± 0.78 (SSMI) | **1.20 ± 0.98**<br>1.37 ± 0.78<br>1.20 ± 0.78<br>1.32 ± 0.98 | |
| T12 (K/decade) | 0.00 ± 0.04 (HIRS) | **0.06 ± 0.04**<br>0.07 ± 0.04<br>0.08 ± 0.04<br>0.06 ± 0.04 | **0.24 ± 0.12**<br>0.24 ± 0.12<br>0.26 ± 0.10<br>0.23 ± 0.12 |
| T2 (K/decade) | 0.17 ± 0.08 (RSS)<br>0.08 ± 0.08 (UAH) | **0.19 ± 0.08**<br>0.19 ± 0.08<br>0.21 ± 0.08<br>0.18 ± 0.08 | |
| T2-T12 (K/decade) | 0.17 ± 0.06 (RSS)<br>0.08 ± 0.06 (UAH) | **0.13 ± 0.08**<br>0.12 ± 0.06<br>0.14 ± 0.06<br>0.13 ± 0.06 | **-0.04 ± 0.04**<br>-0.05 ± 0.06<br>-0.05 ± 0.04<br>-0.05 ± 0.04 |

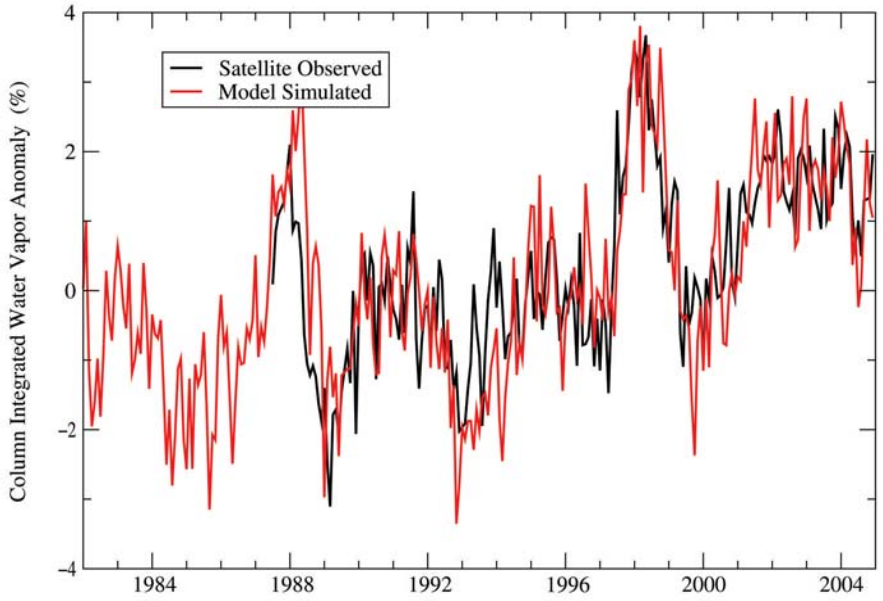
Satellite Observed
Model Simulated
Column Integrated Water Vapor Anomaly (%)
4
2
0
-2
-4
1984
1988
1992
1996
2000
2004

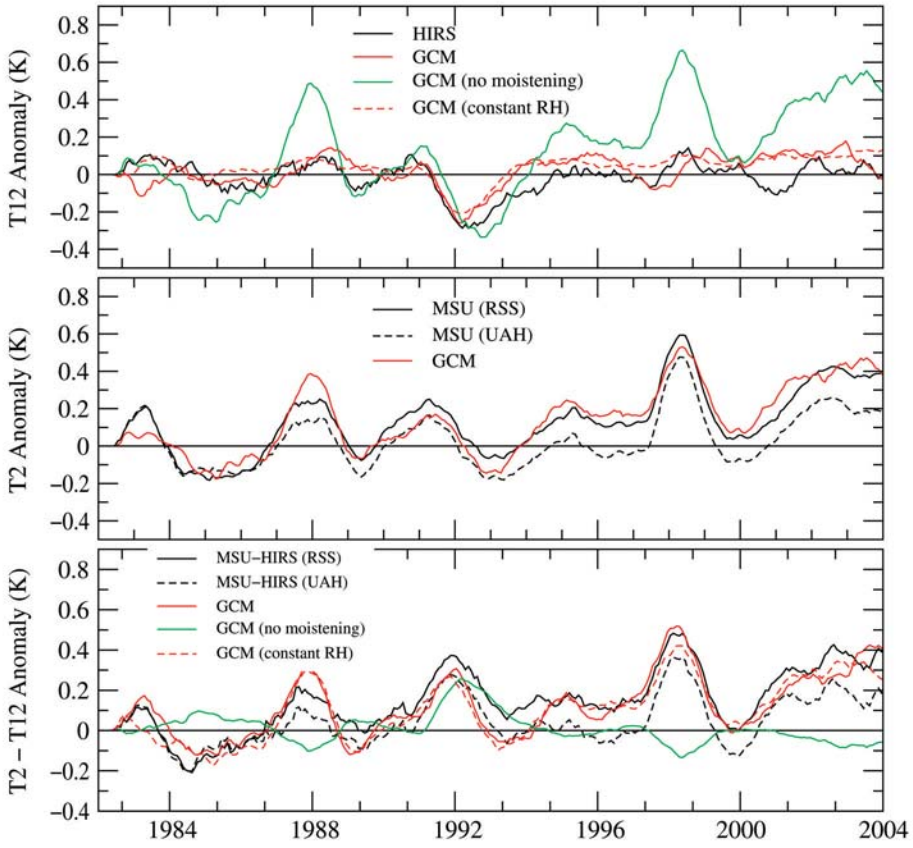
T12 Anomaly (K)
HIRS
GCM
GCM (no moistening)
GCM (constant RH)
T2 Anomaly (K)
MSU (RSS)
MSU (UAH)
GCM
T2 – T12 Anomaly (K)
MSU−HIRS (RSS)
MSU−HIRS (UAH)
GCM
GCM (no moistening)
GCM (constant RH)
0.8
0.6
0.4
0.2
0
−0.2
−0.4
1984
1988
1992
1996
2000
2004

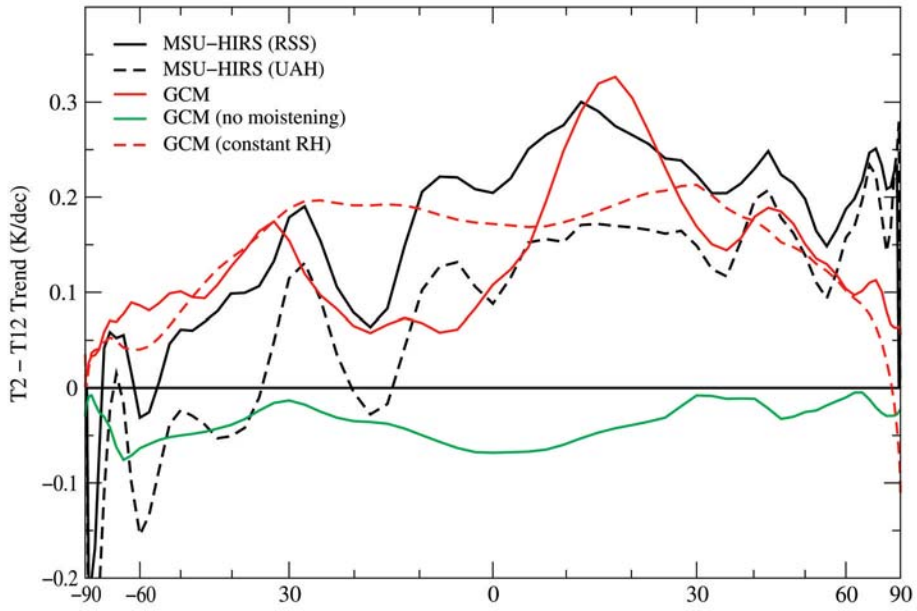
MSU−HIRS (RSS)
MSU−HIRS (UAH)
GCM
GCM (no moistening)
GCM (constant RH)
T2 − T12 Trend (K/dec)
0.3
0.2
0.1
0
−0.1
−0.2
−90
−60
30
0
30
60
90